

# Contact Angle Hysteresis, Adhesion, and Marine Biofouling

Donald L. Schmidt,<sup>†</sup> Robert F. Brady, Jr.,<sup>\*,‡</sup> Karen Lam,<sup>§</sup> Dale C. Schmidt,<sup>†</sup> and Manoj K. Chaudhury<sup>§</sup>

Chemistry Division, Naval Research Laboratory, Washington, D.C. 20375, The Dow Chemical Company, Midland, Michigan 48674, and Department of Chemical Engineering, Lehigh University, Bethlehem, Pennsylvania 18015

Received July 29, 2003. In Final Form: January 9, 2004

Adhesive and marine biofouling release properties of coatings containing surface-oriented perfluoroalkyl groups were investigated. These coatings were prepared by cross-linking a copolymer of 1H,1H,2H,2H-heptadecafluorodecyl acrylate and acrylic acid with a copolymer of poly(2-isopropenyl-2-oxazoline) and methyl methacrylate at different molar ratios. The relationships between contact angle, contact angle hysteresis, adhesion, and marine biofouling were studied. Adhesion was determined by peel tests using pressure-sensitive adhesives. The chemical nature of the surfaces was studied by using X-ray photoelectron spectroscopy. Resistance to marine biofouling of an optimized coating was studied by immersion in seawater and compared to previous, less optimized coatings. The adhesive release properties of the coatings did not correlate well with the surface energies of the coatings estimated from the static and advancing contact angles nor with the amount of fluorine present on the surface. The adhesive properties of the surfaces, however, show a correlation with water receding contact angles and contact angle hysteresis (or wetting hysteresis) resulting from surface penetration and surface reconstruction. Coatings having the best release properties had both the highest cross-link density and the lowest contact angle hysteresis. An optimized coating exhibited unprecedented resistance to marine biofouling. Water contact angle hysteresis appears to correlate with marine biofouling resistance.

## Introduction

Prevention of marine biofouling is a problem of considerable economic importance because biofouling shortens service life and increases operating costs. Many commercial vessels and warships currently use antifouling coatings that minimize the buildup of marine organisms to ship hulls and submarines. Although effective, these coatings contain organometallic compounds that are potentially toxic to marine environments. They are, therefore, subject to current and future environmental regulations. An alternate to these toxic paints would be an environmentally benign coating from which marine organisms could be easily removed.

A surface that would totally resist biofouling has been sought for many years and continues to attract considerable practical and theoretical interest.<sup>1–4</sup> Unfortunately, there is not as yet a surface that completely resists biofouling.<sup>1–3,5</sup> Ideally, the bioadhesion would be weak enough that the weight of the foulant or the hydrodynamic forces created by the ship's motion would dislodge the marine organisms. The intent of the present work is to increase the understanding needed to develop such a coating.

On the basis of one conventional theory of adhesion,<sup>6</sup> it could be assumed that the release property of a material is primarily controlled by its surface free energy of the type that gives rise to water repellency. To reduce biofouling, two types of coatings captured the imagination of researchers: silicones and fluorocarbons. Silicone elastomers have shown promise for combating biofouling, but the performance of fluorocarbon-based coatings has been disappointing.<sup>2</sup> This was a surprising result considering that the surface energy of fluorocarbons ( $\sim 10$ – $18$  mJ/m<sup>2</sup>) is lower than that of silicones ( $\sim 22$  mJ/m<sup>2</sup>). Although surface energy definitely plays an important role in adhesion, other studies have demonstrated that surface energy is not the sole reason for the excellent release properties of low-energy coatings.<sup>6,7</sup> In this study, we have attempted to use wettability measurements and adhesion testing for studying and predicting the release properties of surfaces.

Adhesive interactions between a liquid drop and a solid substrate cause the liquid to spread. Liquid cohesive forces cause the drop to dewet. The contact angle (CA) is determined by the competition between these two forces. CAs are commonly used to determine wettability and to predict adhesion.<sup>6</sup> The static CA,  $\theta_s$ , is obtained by simply placing a liquid drop on a horizontal, flat, nondeformable surface and measuring the angle at the liquid–solid–air boundary. Forcing the liquid to flow yields an advancing angle,  $\theta_a$ , and withdrawing the liquid yields a receding angle,  $\theta_r$ . The surface free energy is generally calculated from static CAs, which are approximately equal to the advancing angles.<sup>8</sup> The difference ( $\theta_a - \theta_r$ ) is related to wetting or CA hysteresis, which is due to the existence of

\* To whom correspondence should be addressed. E-mail: sharonandbobb@aol.com.

<sup>†</sup> The Dow Chemical Company.

<sup>‡</sup> Naval Research Laboratory.

<sup>§</sup> Lehigh University.

(1) Brady, R. F., Jr. *J. Coat. Technol.* **2000**, 72 (900), 44–56.

(2) Brady, R. F., Jr.; Singer, I. L. *Biofouling* **2000**, 15 (1–3), 73–81.

(3) Brady, R. F., Jr. *Chemistry & Industry* **1997**, 219–222.

(4) Swain, G.; Anil, A. C.; Baier, R. E.; Chia, F. S.; Conte, E.; Cook, A.; Hadfield, M.; Haslbeck, E.; Holm, E.; Kavanagh, C.; Kohrs, D.; Kovach, B.; Lee, C.; Mazzella, L.; Meyer, A. E.; Qian, P. Y.; Sawant, S. S.; Schultz, M.; Sigurdsson, J.; Smith, C.; Soo, L.; Terlizzi, A.; Wagh, A.; Zimmerman, R.; Zupo, V. *Biofouling* **2000**, 16, 331–344.

(5) Saroyan, J. R.; Lindler, E.; Dooley, C. A.; Bleile, H. R. *Ind. Eng. Chem. Prod. Res. Dev.* **1970**, 9, 123–128.

(6) Kinlock, A. K. *Adhesion and Adhesives, Science and Technology*; New York: Chapman and Hall, 1987; Chapter 2.

(7) Brady, R. F., Jr. *Prog. Org. Coat.* **1999**, 35, 31–35.

(8) Good, R. J.; van Oss, C. J. In *Modern Approaches to Wettability, Theory and Applications*; Schrader, M. E., Loeb, G. I., Eds.; New York: Plenum Press: 1992; p 24.

metastable states at the solid–liquid–vapor interface and is an indication of a departure from equilibrium.<sup>8–11</sup> In terms of energetics, CA hysteresis (or wetting hysteresis) may also be defined as  $\gamma(\cos \theta_r - \cos \theta_a)$ , where  $\gamma$  is the surface tension (or surface free energy) of the wetting liquid.<sup>9</sup> It implies that the free energy required to separate the liquid from the solid is greater than the energy released during contact.

In this study, we measure the relative wettability of surfaces by a “tilt-angle, sessile drop” technique.<sup>12</sup> The tilt angle (or critical inclination angle),  $\phi$ , is the incline angle of a flat surface at which the trailing edge of a liquid drop of known volume will just begin to move. It is a manifestation of the force required to start the liquid drop in motion. As the tilt angle is increased, the drop elongates and the trailing edge remains stationary until the gravitational force is sufficient to just overcome the adhesion between the liquid and substrate. At the drop’s critical configuration (i.e., at the drop’s first incipient motion), we record  $\phi$  and measure  $\theta_r$  (at the trailing, dewetting edge) and  $\theta_a$  (at the leading, wetting edge). Furmidge<sup>12</sup> derived and demonstrated that a drop at its critical configuration essentially satisfies the relationship  $mg \sin \phi = \omega \gamma (\cos \theta_r - \cos \theta_a)$ , where  $m$  is the mass of the drop,  $g$  is the acceleration of gravity,  $\omega$  is the width of the drop, and  $\gamma$  is the surface tension of the liquid drop. For identical liquid drops,  $\sin \phi$  is proportional to and, thus, a measure of CA hysteresis. This equation indicates that the difference between  $\theta_r$  and  $\theta_a$  and not the absolute values of the angles is the most important factor when studying surface wettability. If there were no hysteresis, a drop would slide or roll off at the slightest tilt of the surface. Ideally the relative adhesion of a solid adhesive to a surface could be predicted by measuring the CA hysteresis of liquids that are chemically similar to the adhesive. The coatings we describe here are unique because there is no perceptible “stick–slip” behavior of the drops during the measurements. The motion of the drops may be stopped and then restarted by changing the tilt angle by even less than 1°. Therefore, the measurements are reproducible to at least  $\pm 1^\circ$ . With these coatings, the plots of drop volume versus  $\sin \phi$  are essentially linear, provided the coatings are first equilibrated with the liquid.

Many previous studies may have failed to find a proper correlation between adhesion and wettability because they focused only on static CAs.<sup>6</sup> Recently, the relationship between adhesion and CA hysteresis has been investigated in some detail with a coating prepared by incorporating a small amount of an alkyl amide functional perfluoropolyether (PFPE) into a siloxane network.<sup>13</sup> The surface energy of the resultant material decreased from 20 to 8 mJ/m<sup>2</sup> as the concentration of PFPE increased from 0 to 1.5%. The adhesive strength of the coating toward an acrylic pressure-sensitive adhesive, however, increased as the surface energy decreased, which is just opposite to that expected from the surface energy hypothesis of adhesion. Advancing and receding CA measurements showed that these surfaces exhibit a pronounced hysteresis, which correlated well with their adhesive properties.

In this paper, the relationship between CA hysteresis and adhesion, measured by peel tests with pressure-

sensitive adhesives,<sup>14</sup> has been developed further by using a previously reported and well-characterized family of perfluoroalkyl-based coatings.<sup>15–17</sup> The nonstick properties of these coatings are related to obtaining surface-oriented CF<sub>3</sub>-terminated perfluoroalkyl groups that form only very weak chemical bonds to adhesives. The particular nonstick coatings we describe here were prepared by cross-linking a copolymer of 1*H*,1*H*,2*H*,2*H*-heptadecafluorodecyl acrylate and acrylic acid with a copolymer of poly(2-isopropenyl-2-oxazoline) and methyl methacrylate. The cross-link density was controlled by varying the molar ratio of the two components. In addition to studying peel adhesion, we have also investigated the relationship between marine biofouling and CA hysteresis. The biofouling of the highly optimized coating was compared to similar but less optimized coatings, which had been previously prepared and studied.<sup>15</sup>

## Experimental Section

Except as specifically described here, the polymer preparations, coating formulations, procedures for application and curing of the coating, and CA measurements were performed as previously reported.<sup>15</sup>

**Preparation of the First Coating.** The coating we refer to in the text as “the first coating” was prepared as described in ref 15 and was based on a 60:40 (weight ratio) of 2-(perfluoroalkyl)-ethyl methacrylate and 2-(perfluoroalkyl)ethyl methacrylate CF<sub>3</sub>–(CF<sub>2</sub>)<sub>*n*</sub>CH<sub>2</sub>CH<sub>2</sub>OC(O)C(CH<sub>3</sub>)=CH<sub>2</sub> [*n* = 3, 5, 7, 9; (*n*) = 7.3], which was obtained from the DuPont Co. Chemicals and Pigments Department (Wilmington, DE) and is commercially known as Zonyl TM, and  $\beta$ -carboxyethyl acrylate, known as Sipomer B-CEA, which was obtained from Rhone-Poulenc (Cranbury, NJ) and is a mixture of acrylic acid oligomers. The copolymer was cross-linked with an 80:20 (weight ratio) of 2-(isopropenyl-2-oxazoline) and methyl methacrylate. The oxazoline IPO monomer used to prepare the cross-linking polymer was obtained from The Dow Chemical Co. (Midland, MI) but is no longer available. The copolymer was prepared by a peroxide-initiated polymerization and purified by dialysis.<sup>15</sup> The coating tested for marine biofouling had a  $M_{\text{carb}}/M_{\text{oxa}} = 1$  and was applied as a 10:10:80 (weight ratio) of a solids, ethylene glycol, and water solution.

**Preparation of the Second (Improved) Coating.** The coating we refer to in the text as the second improved coating was chemically identical to the first coating but it was applied as a 10.3:21.2:5.2:63.3 weight ratio of the solids, ethylene glycol, 1-methyl-2-pyrrolidinone, and water solution. The coating tested for marine biofouling had a  $M_{\text{carb}}/M_{\text{oxa}} = 1$ .

**Preparation of the Third (Optimized) Coating System.** The coating we refer to in the text as the third optimized coating was based on a different perfluoroalkyl acrylate copolymer than the first and second coatings. It was prepared by the continuous and simultaneous addition of three liquid streams under nitrogen at 80 °C for 3 h into a stirred reaction vessel containing Vazo 67 (1.0 g, DuPont Co., Wilmington, DE), propylene glycol (10.0 g), methyl ethyl ketone (25 g), and 1-methyl-2-pyrrolidinone (10.0 g). The first stream contained mercaptoethanol (0.03 g) and methyl ethyl ketone (8.0 g). The second stream contained 1*H*,1*H*,2*H*,2*H*-heptadecafluorodecyl acrylate (31.9 g, Viscoat 17FM, Osaka Organic Chemical Industries, Ltd., Osaka, Japan), acrylic acid (13.7 g), and methyl ethyl ketone (30.0 g). The third stream contained Vazo 67 (1.1 g) and methyl ethyl ketone (8.0 g). After addition was complete, the reaction solution was held at 80 °C for 30 min, and then the polymeric product was isolated, purified, and titrated for carboxylic acid as previously described.<sup>15</sup> The coatings were applied as an 8.8:21.8:4.0:4.0:61.4 (weight

(9) Chaudhury, M. K.; Owen, M. J. *J. Phys. Chem.* **1993**, *97*, 5722.  
 (10) Dettre, R. H.; Johnson, R. E. *J. Phys. Chem.* **1965**, *69*, 1507.  
 (11) Chen, Y. L.; Helm, C. A.; Israelachvili, J. N. *J. Phys. Chem.* **1993**, *97*, 4128.  
 (12) Furmidge, C. G. L. *J. Colloid Sci.* **1962**, *17*, 309.  
 (13) Thanawala, S. K.; Chaudhury, M. K. *Langmuir* **2000**, *12*, 1256–1260.

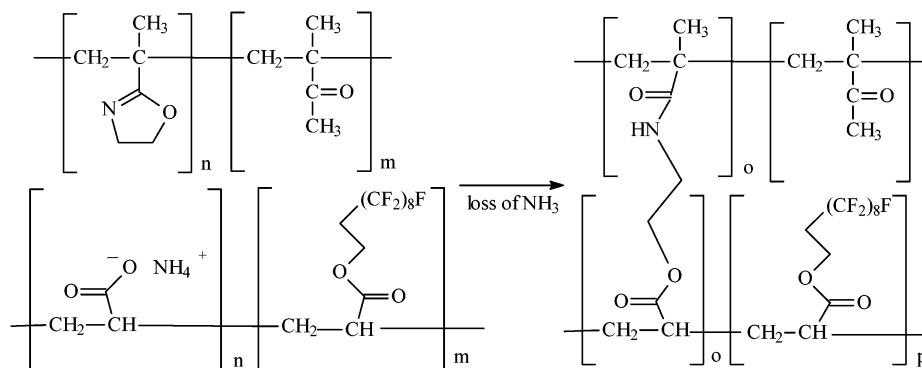
(14) Newby, B. Z.; Chaudhury, M. K.; Brown, H. R. *Science* **1995**, *269*, 1407.

(15) Schmidt, D. L.; DeKoven, B. M.; Coburn, C. E.; Potter, G. E.; Meyers, G. F.; Fischer, D. A. *Langmuir* **1996**, *12*, 518.

(16) Lin, J.; Zhu, S.; Swanson, D. R.; Milki, L. *Langmuir* **1996**, *12*, 6676–6680.

(17) Schmidt, D. L.; Coburn, C. E.; DeKoven, B. M.; Potter, G. E.; Meyers, F. M.; Fisher, D. A. *Nature* **1994**, *368*, 39.

Scheme 1



ratio) of the solids, ethylene glycol, 1-methyl-2-pyrrolidinone, propylene glycol, and water solution.

#### Formulation, Application, and Curing of the Coatings.

Two aqueous solutions were used to form the final formulations. The first solution contained the perfluoroalkyl acrylate copolymer of known carboxylic acid activity. The second solution contained an 80:20 (weight ratio) copolymer of poly(2-isopropenyl-2-oxazoline) and methyl methacrylate of known oxazoline activity determined by elemental analysis.<sup>15</sup> The solutions were combined in the ratios needed to yield the desired amount of cross-linking. The final coating formulations contained between 8 and 10% solids. The organic solvents were added to the oxazoline solution followed by the addition of the perfluoroacrylate solutions, which constitutes the final formulation. The proper cosolvents are required to obtain the best nonstick coatings. For CA measurements, the coatings were cast on microscope slides and cured in an oven at 105 °C for 12 h under initially high humidity by placing them in a crystallizing dish containing wet Kemwipe Ex-L Wipers (Kimberly Clark Corp., Roswell, GA) and covering the dish with a watch glass.<sup>15</sup>

For biofouling resistance testing, mild steel panels, 150 × 75 × 3 mm, were roughened, cleaned, coated with a 75- $\mu$ m-thick film of a two-component epoxy-polyamide marine primer, and allowed to cure for 14 days. Before being coated with a fluorinated coating, panels were heated in an oven at 105 °C for 12 h, cleaned with a 5 wt % solution of Joy detergent, rinsed with distilled water, rinsed with 2-propanol, coated with a 25 wt % solution of aryl cyclic sulfonium zwitterion,<sup>18</sup> and then cured at 100 °C for 12 h. After removal from the oven, the panels were cleaned with 2-propanol and immediately coated as just described with a formulation of the perfluoroacrylate polymer and the polyoxazoline cross-linking agent. The final coatings were cured under high humidity at 105 °C for 12 h.

**Resistance to Marine Biofouling.** Panels were tested in the Chesapeake Bay at Deale, MD, as part of a 10-year-old collaborative research program conducted by the Australian, Canadian, and U.S. Navies. Marine growth is variable, and the evaluations are subjective and qualitative, but in experienced hands the results have been very reproducible.<sup>19</sup> Duplicate panels were used for each coating and were immersed to a depth of 0.3–1.3 m (depending on the tides). Fouling was assessed at roughly 1-month intervals during the local fouling season from April to October as follows. Immediately after removal from the water, the attachment of barnacles and clams, bryozoans, worms, slime and algae, and mud was separately assessed as none, trace, slight, medium, mostly covered, or covered. The panels were then cleaned using various methods, and the ease of cleaning was evaluated using the following criteria: no cleaning required, garden hose (15 psi water), easy with sponge or brush, moderate effort with sponge or brush, some scraping required, moderate to strong scraping required, or difficult even with scraping. After cleaning, staining and fouling that could not be removed were

assessed as none, trace, slight, medium, mostly covered, or covered. Finally, the integrity of the cleaned coating was evaluated as excellent, trace defects, few defects, many defects, patches of coating missing, or coating removed from panel. Each panel was photographed before and after cleaning. Poly(methyl methacrylate) was used as a control to assess the viability of the fouling organisms.

**CA and Tilt Angle Measurements.** After curing, the samples were cleaned with a 5% weight solution of Joy detergent and rinsed with distilled water. The measurements were made immediately after the samples had been equilibrated by immersion in water or hexadecane for 12 h. The CAs,  $\theta$ , and tilt angles,  $\phi$ , were obtained at 23 °C using a ramé-hart model A-100 goniometer, equipped with a tilting base (Mountain Lakes, NJ). The liquid drops were applied with a Hamilton microliter gastight syringe (Reno, NV). At the first incipient motion, we record the tilt angle,  $\phi$ , and measure the receding angle,  $\theta_r$ , at the trailing, dewetting edge and the advancing angle,  $\theta_a$ , at the leading, wetting edge. The CA measurements<sup>15</sup> are reproducible to  $\pm 2^\circ$ . The tilt angles are reproducible to  $\pm 1^\circ$ . Measurements were made using 5- $\mu$ L drops of hexadecane and 50- $\mu$ L drops of distilled water. For these coatings, our plots of drop volume versus  $\sin \phi$  are essentially linear for drops of water between 20 and 70  $\mu$ L and hexadecane between 3 and 10  $\mu$ L.<sup>15</sup>

**Adhesion Measurements.** Peel fracture energies of an acrylic pressure-sensitive adhesive (3M brand Scotch Tape) on these surfaces were measured as a function of the peel velocity.<sup>14</sup> These measurements were carried out using a 90° peel configuration by hanging dead loads on the free end of the adhesive tape. As the crack propagated, the peel velocity was estimated by measuring the length of tape that peeled away within a certain time. Peel velocities increased with peel force for each coating. These data were interpolated to obtain the peel force at a given peel velocity (500  $\mu$ m/s) for all surfaces. The length of time that the tape was in contact with the surface seemed to have a negligible effect on the measured value of the peel velocity. The fracture energy is reproducible to  $\pm 3$  J/m<sup>2</sup>.

**X-ray Photoelectron Spectroscopy (XPS).** The surface compositions of the coatings were determined by XPS using a Scienta ESCA-300. X-rays were generated using a water-cooled high-intensity Al K $\alpha$  anode at a power of 4.5 kW. The spectra were acquired at a 90° takeoff angle using a pass energy of 150 eV. An electron flood gun was used to minimize charging of the samples.

## Results and Discussions

**Chemistry.** The cross-linking of the final films takes place by the reaction of the ammonium carboxylate functional group on the perfluoroalkyl polymer with the oxazoline-based cross-linking agent.<sup>16</sup> Both materials are stable until applied to a substrate and heated. Upon heating and loss of solvent and ammonia, the carboxylic acid functionality reacts with the oxazoline to form an amide ester cross-link, as shown in Scheme 1. There is a decrease in hydrophilicity as a result of the loss of both the carboxylic acid and the oxazoline functionalities but

(18) Hill, L. W.; Rondan, N.; Schmidt, D. L. *Macromolecules* **2001**, *34*, 372–375.

(19) Lewis, J. A.; Foster, T.; Brady, R. F., Jr. *Environmentally Acceptable Flexible Fouling Release or Prevention Coatings*, Report TTCP-MAT-TP-6-09; Defense Science and Research Organization: Melbourne, June, 1997.

some increase in hydrophilicity as a result of the formation of amide functionality.

The cross-link density of the final coatings was adjusted by combining various ratios of the reactants to yield the desired carboxylate-to-oxazoline molar ratios denoted by  $M_{\text{carb}}/M_{\text{oxa}}$  throughout the text. At equal molar ratios, when  $M_{\text{carb}}/M_{\text{oxa}} = 1$ , the cross-linking should be at a maximum and the polarity should be at a minimum because there is sufficient oxazoline functionality to react with all of the carboxylic acid groups. As  $M_{\text{carb}}/M_{\text{oxa}}$  decreases below 1, cross-linking decreases and polarity increases as a result of an increase in hydrophilic oxazoline functionality. As  $M_{\text{carb}}/M_{\text{oxa}}$  increases above 1, cross-linking decreases and polarity increases as a result of an excess of hydrophilic carboxylic acid functionality. The total fluorine content also increases with increasing  $M_{\text{carb}}/M_{\text{oxa}}$ .

**Wettability and Adhesion.** When a polar liquid such as water contacts a polymeric surface, polar molecules in the region of the surface will rearrange or reconstruct, allow solvent penetration, and facilitate the migration of polar groups toward the water–polymer interface. For example, pendant hydroxyl groups on a polymer chain will be oriented and buried away from the solid–gas interface. However, because of the strong interaction with water at the solid–water interface, the hydroxyl groups will cause surface reconstruction, which will result in the formation of interfacial, hydroxyl hydrogen bonds with water. A nonpolar liquid, such as a hydrocarbon, does not strongly interact with the polar portions of a surface but interacts more strongly with hydrocarbon-type surface functionality through dispersion forces. The interaction results in increased solvent penetration into the surface and, consequently, reorientation of pendant alkyl functionality toward the liquid hydrocarbon–solid interface. The temperature-driven tendency for a wetting liquid to penetrate into the surface and produce surface reconstruction causes an increase in the free energy of interaction, which is added to the work of adhesion.<sup>20</sup> Cross-linking inhibits liquid penetration and surface reconstruction by immobilizing the surface molecules and, consequently, lowers the difference in the amount of energy released during contact and separation (wetting and dewetting of the surface). Cross-linking of a polymeric surface should, therefore, decrease CA hysteresis.

We used the tilt angles and CAs of water and hexadecane to monitor the polar and dispersion character of the surfaces. The wetting measurements we report here were made immediately after equilibrating the samples in water or hexadecane for about 12 h. If the samples are not first equilibrated, the hystereses are considerably lower.<sup>15</sup> Peel fracture energies of an acrylic pressure-sensitive adhesive were measured to obtain a correlation with CA hysteresis.

Figure 1 is a plot of the advancing,  $\theta_a$ , and receding,  $\theta_r$ , angles of water and peel fracture energy versus  $M_{\text{carb}}/M_{\text{oxa}}$ . To simplify the comparison of the data, the y axis for the peel fracture energy in Figures 1 and 2 is inverted. Because the receding angles for water are most sensitive to the polar character<sup>11</sup> and cross-link density of the surface, there is a definite water  $\theta_r$  maximum at about  $M_{\text{carb}}/M_{\text{oxa}} = 1.0$ . The receding angle increases from  $M_{\text{carb}}/M_{\text{oxa}} = 0.3$  to  $M_{\text{carb}}/M_{\text{oxa}} = 1.2$  and decreases sharply at  $M_{\text{carb}}/M_{\text{oxa}}$  values greater than 1.2, indicating the sensitivity of  $\theta_r$  to surface polarity and decreasing cross-link density. The advancing angles are larger than the receding angles and are the most sensitive to the nonwetable portions of a surface. There is an increase in  $\theta_a$  between

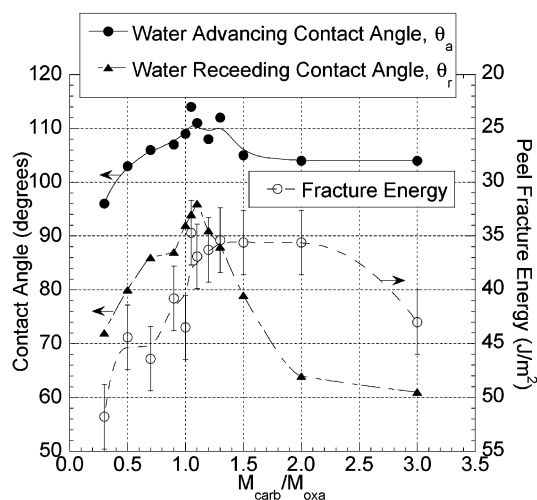


**Figure 1.** Plot of the advancing,  $\theta_a$ , and receding,  $\theta_r$ , angles of water and peel fracture energy versus  $M_{\text{carb}}/M_{\text{oxa}}$ . The peel fracture energy is inverted to simplify the comparison of the data.

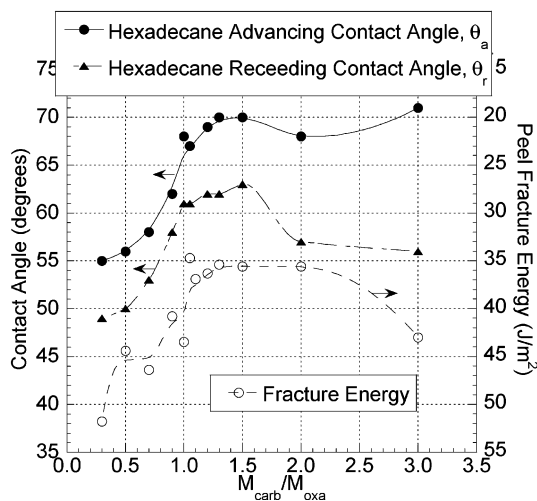


**Figure 2.** Plot of the advancing and receding CAs of hexadecane and peel fracture energy versus  $M_{\text{carb}}/M_{\text{oxa}}$ . The peel fracture energy is inverted to simplify the comparison of the data.

$M_{\text{carb}}/M_{\text{oxa}} = 0.3$  and  $M_{\text{carb}}/M_{\text{oxa}} = 1.1$ , which is consistent with both an increasing cross-link density and an increasing surface concentration of perfluoroalkyl groups. There is no definite  $\theta_a$  maximum in the region of  $M_{\text{carb}}/M_{\text{oxa}} = 1.0$ , but the highest values are between 1.0 and 1.3. There is no significant change in the  $\theta_a$  slope between  $M_{\text{carb}}/M_{\text{oxa}} = 1.5$  and  $M_{\text{carb}}/M_{\text{oxa}} = 3.0$ , which is consistent with little change in the hydrophobic nature of the surfaces, yet the bulk cross-link density decreases and the total bulk perfluoroalkyl content increases. The peel fracture energy, Figure 1, decreases from  $M_{\text{carb}}/M_{\text{oxa}} = 0.3$  to  $M_{\text{carb}}/M_{\text{oxa}} = 1.3$ , which is consistent with increasing cross-linking, decreasing surface polarity, and increasing surface perfluoroalkyl density. Beginning at  $M_{\text{carb}}/M_{\text{oxa}}$  values above about 2.0, the fracture energy (or adhesion) increases, yet the total fluorine content of the coating also increases. The increased fluorine content might be expected to cause a decrease rather than an increase in adhesion.

Because the wettability of hexadecane is more sensitive to the nonpolar (dispersion) character of a surface than to the polar character, increasing surface hydrocarbon content should decrease  $\theta_a$ . Alkylation of a similar coating<sup>15</sup> caused a decrease in the hexadecane receding angles and

(20) Johnson, R. E.; Dettre, R. H. In *Wettability*; Berg, J. C., Ed.; Marcel Dekker: New York, 1993; Chapter 1.

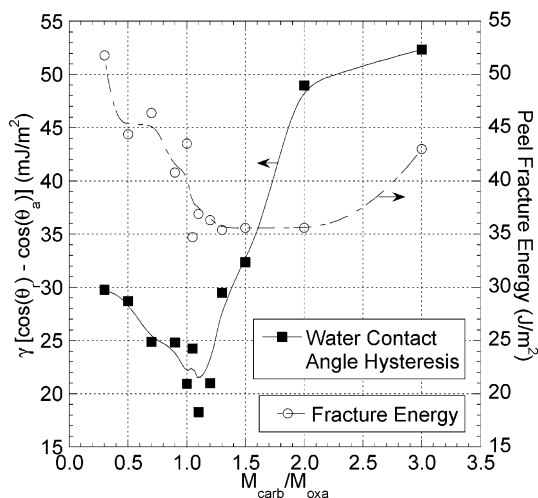


**Figure 3.** Plot of calculated CA hysteresis  $\gamma(\cos \theta_r - \cos \theta_a)$  for water and peel fracture energy versus  $M_{carb}/M_{oxa}$ .

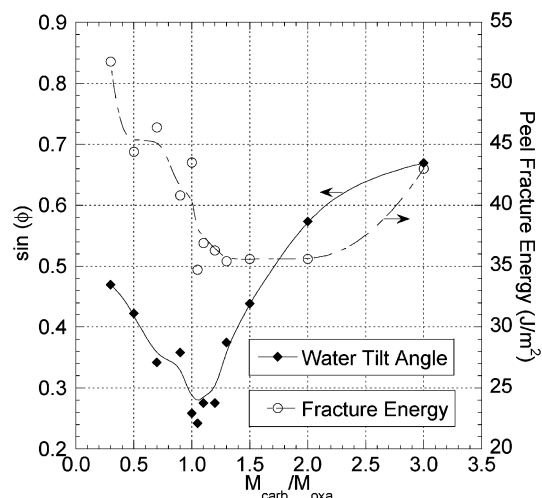
increased the CA hysteresis. Thus, hexadecane wettability should increase with increasing surface hydrocarbon content and decrease with increasing surface perfluoroalkyl content.

Figure 2 is a plot of the advancing and receding CAs of hexadecane and peel fracture energy versus  $M_{carb}/M_{oxa}$ . The receding angles, Figure 2, of hexadecane increase from  $M_{carb}/M_{oxa}$  values of 0.3 to  $M_{carb}/M_{oxa}$  values of 1.5, which is consistent with decreasing hydrocarbon content and increasing cross-linking. The receding angles decrease from between  $M_{carb}/M_{oxa} = 1.5$  to  $M_{carb}/M_{oxa} = 3.0$ . The reason for this decrease in  $\theta_r$  is not obvious from the data plotted in Figure 2. The advancing CAs for hexadecane increase until  $M_{carb}/M_{oxa}$  values become greater than 1.5 but then remain relatively constant at a  $\theta_a$  of about  $70^\circ$  up to  $M_{carb}/M_{oxa} = 3.0$ . A plausible explanation is that, although the total, bulk fluorine content increases with  $M_{carb}/M_{oxa}$ , the surface density of surface-oriented, packed, perfluoroalkyl groups reaches a maximum and remains relatively constant. The peel fracture energy, Figure 2, decreases as both  $\theta_r$  and  $\theta_a$  increase between  $M_{carb}/M_{oxa} = 0.3$  and  $M_{carb}/M_{oxa} = 1.5$ . There is perhaps a weak correlation between peel fracture energy and hexadecane receding CA between  $M_{carb}/M_{oxa} = 1.5$  and  $M_{carb}/M_{oxa} = 3.0$ .

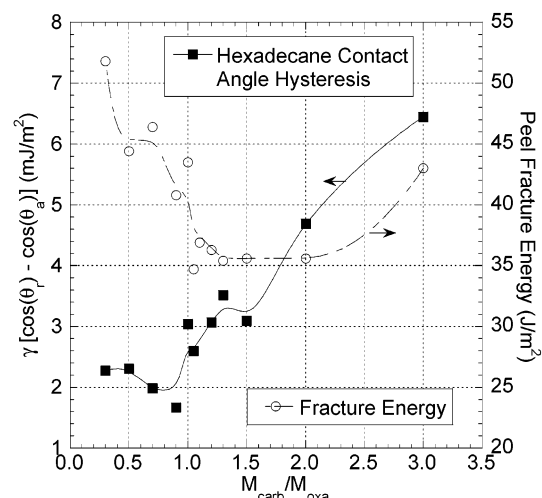
The calculated CA hysteresis,  $\gamma(\cos \theta_r - \cos \theta_a)$ , for water and the peel fracture energy are plotted versus  $M_{carb}/M_{oxa}$  in Figure 3. The CA hysteresis has a sharp minimum at a  $M_{carb}/M_{oxa}$  value of about 1.1, which represents the highest cross-link density and, thus, the lowest water wettability. The peel fracture energy versus  $M_{carb}/M_{oxa}$  is consistent with the change in hysteresis, which increases with increasing degree of adhesion to the surface.

Figure 4 is a plot of the measured CA hysteresis of water plotted as  $\sin \phi$  (where  $\phi =$  tilt angle) and peel fracture energy versus  $M_{carb}/M_{oxa}$ . It is obvious that similar conclusions can be drawn from both Figure 3 and Figure 4.

Figure 5 is a plot of the CA hysteresis expressed as  $\gamma(\cos \theta_r - \cos \theta_a)$  of hexadecane and peel fracture energy versus  $M_{carb}/M_{oxa}$ . It is important to note that the CA hysteresis decreases slightly from  $M_{carb}/M_{oxa} = 0.3$  to  $M_{carb}/M_{oxa} = 0.9$  but then markedly increases from  $M_{carb}/M_{oxa} = 1.0$  to  $M_{carb}/M_{oxa} = 3.0$ , which is consistent with an increase in peel fracture energy. It is significant that the advancing CA of hexadecane (Figure 2) does not increase above  $70^\circ$  between  $M_{carb}/M_{oxa} = 1.2$  and  $M_{carb}/M_{oxa} = 3.0$ . This is consistent with the lack of any significant increase



**Figure 4.** Plot of the measured CA hysteresis of water plotted as  $\sin \phi$  (where  $\phi =$  tilt angle) and peel fracture energy versus  $M_{carb}/M_{oxa}$ .



**Figure 5.** Plot of the calculated CA hysteresis  $\gamma(\cos \theta_r - \cos \theta_a)$  of hexadecane and peel fracture energy versus  $M_{carb}/M_{oxa}$ .

or decrease in the density or orientation of perfluoroalkyl groups on the surface, but there is, however, a definite increase in both CA hysteresis and peel fracture energy between  $M_{carb}/M_{oxa} = 1.2$  and  $M_{carb}/M_{oxa} = 3.0$ . Thus, CA hysteresis appears to be a direct indication of the cross-link density and the resistance to surface penetration and reconstruction when contacted with a liquid. By comparing Figures 1 and 2 with Figure 5, it is obvious that the wettability and release (peel fracture energy) properties of these surfaces cannot be predicted by obtaining advancing CAs alone. However, measuring advancing and receding angles and CA hysteresis does help define the nonstick or release nature of these surfaces.

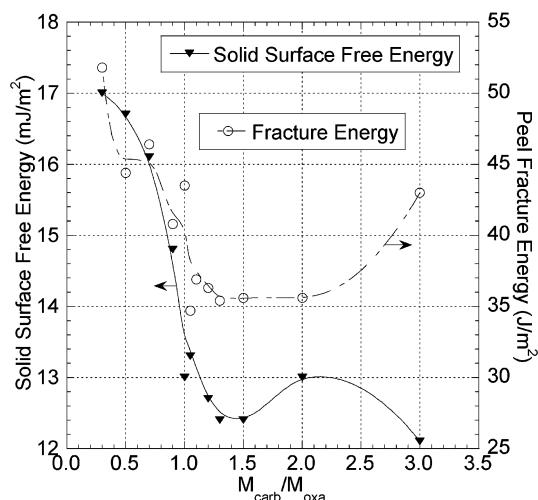
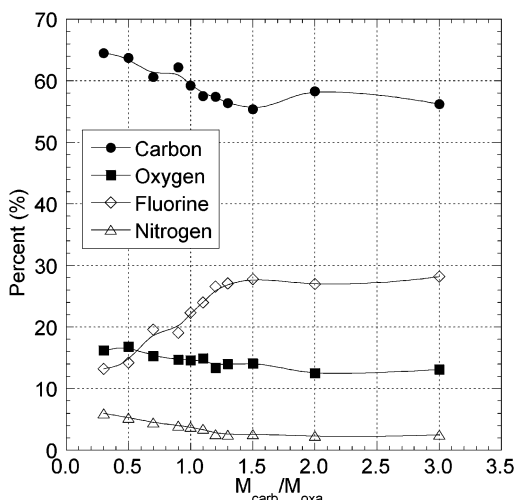
Figure 6 is a plot of peel fracture energy and surface free energy, calculated from the Good–Girifalco–Fowkes equation<sup>21,22</sup> using hexadecane advancing angles, as a function of  $M_{carb}/M_{oxa}$ . Both surface free energy and peel fracture energy decreases from  $M_{carb}/M_{oxa} = 0.30$  to  $M_{carb}/M_{oxa} = 1.5$ . The surface free energy at  $M_{carb}/M_{oxa}$  values greater than 1.5 does not increase, but peel fracture energy does increase. Thus, surface free energy does not adequately predict adhesion.

(21) Fowkes, F. M. *Ind. Eng. Chem.* **1964**, *56*, 40–52.

(22) Good, R. J.; Girifalco, L. A. *J. Phys. Chem.* **1960**, *64*, 561–565.

**Table 1. Comparative Marine Immersion Test Data for Perfluoroalkyl-Based Release Coatings**

coating	season tested	extent of coverage	type of organism	ease of cleaning	residual staining	film integrity
first	1996–1997	covered	bryozoans, slime, algae, barnacles	scraping	medium	few defects
second (improved)	1997	mostly covered	slime, algae, barnacles	light scraping	slight	trace defects
third (optimized)	1998–2000	slight	slime, algae, barnacles	garden hose	none	no defects

**Figure 6.** Plot of peel fracture energy and surface free energy, calculated from the Good–Girifalco–Fowkes equation, using hexadecane advancing angles, as a function of  $M_{\text{carb}}/M_{\text{oxa}}$ .**Figure 7.** Plot of percent composition obtained from the XPS of the surface carbon, fluorine, oxygen, and nitrogen versus  $M_{\text{carb}}/M_{\text{oxa}}$  using a takeoff angle of  $90^\circ$ .

**XPS.** Figure 7 is a plot of percent composition of surface carbon, fluorine, oxygen, and nitrogen versus  $M_{\text{carb}}/M_{\text{oxa}}$  using a takeoff angle of  $90^\circ$ . Some radiation-induced degradation was apparent and may have decreased the measured fluorine content for all the samples.<sup>23</sup> The percent fluorine at the surface increases from  $M_{\text{carb}}/M_{\text{oxa}} = 0.5$  to  $M_{\text{carb}}/M_{\text{oxa}} = 1.5$  and then stays constant up to  $M_{\text{carb}}/M_{\text{oxa}} = 3.0$ . This is very consistent with the advancing angles of hexadecane (Figure 2), which stay relatively constant at  $70^\circ$  for  $M_{\text{carb}}/M_{\text{oxa}}$  greater than 1.5. Thus, the perfluoroalkyl surface concentration reaches a saturation value or a critical packing density of the surface perfluoroalkyl groups. The advancing angle of water, Figure 1, at  $M_{\text{carb}}/M_{\text{oxa}}$  greater than 1.5 also suggests the surface has a high concentration of perfluoroalkyl groups. A second study used a takeoff angle of  $15^\circ$  to measure concentrations

**Table 2. Water CAs and CA Hysteresis for Release Coatings Tested in Table 1**

coating	season tested	water advancing CA ( $\theta_a$ )	water receding CA ( $\theta_r$ )	CA hysteresis ( $\sin \phi$ )
first	1996–1997	91	72	0.43
second (improved)	1997	117	93	0.29
third (optimized)	1998–2000	111	91	0.24

at a shallower depth and found that the concentration of fluorine at the surface was higher than that detected using a takeoff angle of  $90^\circ$ . It is significant that more surface fluorine is detected at  $15^\circ$  than at  $90^\circ$ , indicating that there is considerable surface enrichment of fluorine.

The decrease in peel fracture energy from  $M_{\text{carb}}/M_{\text{oxa}} = 0.30$  to  $M_{\text{carb}}/M_{\text{oxa}} =$  about 1.3 can be rationalized from the receding CAs and surface free energy (Figures 1, 2, and 6). The increase in peel fracture energy at  $M_{\text{carb}}/M_{\text{oxa}}$  greater than 2.0 cannot. The receding angles, Figures 1 and 2, and XPS, Figure 7, indicate that at  $M_{\text{carb}}/M_{\text{oxa}}$  greater than 1.5 the surfaces contain tightly packed and surface-oriented perfluoroalkyl groups. If this is the case, then the adhesion to these surfaces should be very low. To establish adhesion, the pressure-sensitive adhesive must induce molecular reconstruction. This is consistent with the plots of CA hysteresis in Figures 3–5, which indicate that surface penetration and reconstruction occurs when exposed to water and hexadecane.

**Marine Biofouling.** The marine biofouling resistance of the optimized coating we describe here was compared with two similar and previously reported perfluoro-based coatings. All these coatings had  $M_{\text{carb}}/M_{\text{oxa}} = 1$ . The first coating was described in detail in ref 15 and was tested in 1996. A second improved coating system<sup>24</sup> was prepared by adding 1-methyl-2-pyrrolidinone in addition to ethylene glycol used in the previous formulation.<sup>15</sup> This second coating was evaluated for marine biofouling in 1997.

The third and optimized coating we describe here was tested in 1998, and the chemistry is shown in Scheme 1. Optimization was accomplished by using a pure sample of the perfluoroacrylate monomer and an optimized solvent combination in the coating formulation. The ratio of fluorine to carboxylic acid was higher in this optimized coating than in the first two coatings.

The time of immersion that caused fouling sufficient that it could not be removed by a stream of water from a garden hose was 1 month for the 1996 sample,<sup>24</sup> 3 months for the 1997 sample, and greater than 7 months for the 1998 sample. A more detailed comparison of these three coatings is illustrated in Table 1. The water advancing and receding CAs and the CA hystereses of these coatings are reported in Table 2. While the water CA hysteresis correlated with marine biofouling, the water advancing and receding CAs did not. The hexadecane CA hysteresis also did not correlate with marine biofouling. This lack of correlation with hexadecane could be related to the highly polar nature of the fouling organisms.

The marine biofouling resistances of the present coatings were compared with several hundred panels of

(23) Chaney, R.; Barth, G. Z. *Anal. Chem.* **1987**, *329*, 143–146.(24) Brady, R. F., Jr.; Bonafede, S. J.; Schmidt, D. L. *Surf. Coat. Int.* **1999**, *82* (12), 582–585.

commercial and experimental nontoxic antifouling coatings. This coating accumulated less fouling and accumulated it slower than all other coatings we tested. Slime and algae fouling were slight; both were present throughout the season but were easily removed with a garden hose. Barnacle fouling was rated as trace; small barnacles were able to attach, but only early in the fouling season when growth was most vigorous. If the small barnacles were not dislodged by a stream of water from a garden hose, they were allowed to remain on the coating until the next monthly inspection. All barnacles fell off the coating before they grew to be 8 mm in diameter. Cleaning never required more than a stream of water from a garden hose. There was no fouling or staining that could not be removed. The coatings were easily restored to their before-immersion condition, and the coatings did not decompose, delaminate, or sustain mechanical damage during testing.

**Surface Restructuring and Hysteresis.** Previous studies<sup>15</sup> of these surfaces using atomic force microscopy indicated that the observed CA hysteresis was not related to surface roughness. These earlier studies, using similar coatings, indicated that the amount of change in CA hysteresis during immersion in water or hexadecane was dependent upon two factors: the deviation of  $M_{\text{carb}}/M_{\text{oxa}}$  from 1, reflecting the change in cross-linking and chemical functionality, and the time the surface was exposed to the test liquid. The farther that  $M_{\text{carb}}/M_{\text{oxa}}$  deviated from 1, the more and the faster the hysteresis changed. Even at  $M_{\text{carb}}/M_{\text{oxa}} = 1$ , there was a small change in hysteresis. In this work, hysteresis was measured after equilibrating the surface in the test liquid for 12 h. The unprecedented resistance to marine biofouling at  $M_{\text{carb}}/M_{\text{oxa}} = 1$  appears to be related to low CA hysteresis, which is due to immobilized, closely packed, oriented  $\text{CF}_3$ -terminated perfluoroalkyl groups. At optimum cross-linking,  $M_{\text{carb}}/M_{\text{oxa}} = 1$ , the surface is not only less polar in nature but also the surface molecules are more immobilized and, thus, are less affected by solvent. Therefore, there is less change

in wettability after equilibrating with the test liquid. The cross-linking deters liquid penetration into the surface and consequent reconstruction of the atoms and molecules at the surface of the substrate. For the same reasons, cross-linking also decreases the adhesion of marine organisms. When a protein-rich marine adhesive comes in contact with a cross-linked surface, the tendency for the molecules of the adhesive to penetrate through the outermost molecules on the substrate surface is reduced and interaction with the residual polar groups is greatly diminished. Our conclusions are consistent with careful studies by others who have shown a strong correlation of surface reconstruction of fluorinated surfaces to surface energy<sup>25</sup> and CA hysteresis.<sup>26</sup>

### Conclusions

This study indicates that the release properties of low-energy surfaces cannot be predicted by using only static or advancing CAs. A better prediction of release properties can be obtained by using both advancing and receding CAs and CA hysteresis. These measurements should be conducted immediately after equilibrating the surface in the test liquids. The coatings that we studied that had the best overall release properties had both the highest cross-link density and highest receding angles and the lowest CA hysteresis. CA hysteresis appears to be a direct indication of the resistance to liquid or adhesive surface penetration and reconstruction. An optimized coating having both low water CA hysteresis and high receding CA exhibited unprecedented resistance to marine biofouling.

**Acknowledgment.** We are indebted to Gene D. Rose for his many helpful conversations and suggestions.

LA035385O

(25) Perutz, S.; Wang, J.; Kramer, E. J.; Ober, C. K. *Macromolecules* **1998**, *31*, 4272–4276.

(26) Katano, Y.; Tomono, H.; Najima, T. *Macromolecules* **1994**, *27*, 2342–4276.